CONVERGENCE PROPERTIES OF QUASICLASSICAL TRAJECTORY CALCULATIONS ON DYNAMICS OF AUTOIONIZATION EVENT IN $He(2^3S)$–D_2 PENNING IONIZATION

Jan VOJTIK[a] and Richard KOTAL[b]

[a] *J. Heyrovsky Institute of Physical Chemistry, Academy of Sciences of the Czech Republic, 182 23 Prague 8, Czech Republic; e-mail: vojtik@jh-inst.cas.cz*

[b] *Department of Physical and Macromolecular Chemistry, Faculty of Science, Charles University, 128 40 Prague 2, Czech Republic; e-mail: kotal@dirac.jh-inst.cas.cz*

Received October 11, 1996
Accepted December 2, 1996

Dedicated to Dr Karel Mach on the occasion of his 60th birthday.

An analysis of the degree of convergence of theoretical pictures of the dynamics of the autoionization event $He(2^3S)$–$D_2(v'' = 0) \rightarrow [He\ldots D_2^+(v')] + e$ is presented for a number of batches of Monte Carlo calculations differing in the number of the trajectories run. The treatment of the dynamics consists in 2D classical trajectory calculations based on static characteristics which include a quantum mechanical treatment of the perturbed $D_2(v'' = 0)$ and $D_2^+(v')$ vibrational motion. The vibrational populations are dynamical averages over the local widths of the $He(2^3S)$–$D_2(v'' = 0)$ state with respect to autoionization to $D_2^+(\ldots He)$ in its v'th vibrational level and the Penning electron energies are related to the local differences between the energies of the corresponding perturbed $D_2(v'' = 0)(\ldots He^*)$ and $D_2^+(v')(\ldots He)$ vibrational states. Special attention is paid to the connection between the requirements on the degree of convergence of the classical trajectory picture of the event and the purpose of the calculations. Information is obtained regarding a scale of the trajectory calculations required for physically sensible applications of the model to an interpretation of different type of experiments on the system: total ionization cross section measurements, Penning ionization electron spectra, subsequent 3D classical trajectory calculations of branching ratios of the products of the postionization collision process, and interpretation of electron ion coincidence measurements of the product branching ratios for individual vibrational levels of the nascent Penning ion.

Key words: Convergence of trajectory calculations; Penning ionization; Nascent Penning ion.

In our recent paper[1] we reported a theoretical picture of the dynamics of the autoionization event

$$He(2^3S) + D_2(v'' = 0) \rightarrow [He\ldots D_2^+(v')] + e\ . \qquad (1)$$

The treatment of the dynamics used in this study consisted in 2D classical trajectory calculations based on static characteristics which include quantum mechanical treatment of the perturbed $D_2(v'' = 0)$ and $D_2^+(v')$ vibrational motion. The main objective of our earlier paper[1] was to theoretically simulate the Penning ionization electron spectra (PIES) of the $He(2^3S)$–$D_2(v'' = 0)$ system and compare them with the experimental ones, recently obtained from crossed supersonic molecular beams PIES measurements[2]. The main result of our theoretical effort is shown in Table I. Even a cursory examination of this table reveals that our calculations were successful in that they eliminated some uncertainties in the experimental PIES data, the resulting set of theoretical nascent Penning ion populations being more complete than its experimental counterpart. One of the reasons for the success of the calculations can be ascribed to that the theoretical simulation of the PIES spectra was based on very extended calculations. More specifically, 2 500 000 trajectories were run to obtain sufficiently converged sets of Penning electron energies and vibrational population factors corresponding to the nascent Penning ions $[He\ldots D_2^+(v')]$ in individual vibrational levels.

It is to be noted in this connection that $He(2^3S)$–D_2 belongs to a class of atom–diatom autoionizing collision systems with repulsive interaction and, further, that the collision

TABLE I

Calculated vibrational population factors $P_{v'}$ (normalized to 100 at $v' = 3$) and average energies $E_{v'}$ (in eV) in Penning ionization of $He(2^3S) + D_2(v'' = 0) \rightarrow [He\ldots D_2^+] + e$

v′	$P_{v'}$[a]	$P_{v'}$(exp)[b]	$E_{v'}$[a]	v′	$P_{v'}$[a]	$P_{v'}$(exp)[b]	$E_{v'}$[a]
0	26.31	21 ± 8	4.378	13	7.27	–	2.395
1	62.75	59 ± 12	4.179	14	4.55	–	2.291
2	90.47	89 ± 15	3.989	15	3.13	–	2.196
3	100.00	100	3.808	16	2.43	–	2.109
4	95.09	94 ± 16	3.634	17	1.87	–	2.032
5	81.18	80 ± 14	3.467	18	1.27	–	1.957
6	63.08	74 ± 12	3.308	19	0.96	–	1.894
7	50.00	49 ± 9	3.157	20	0.72	–	1.843
8	36.73	33 ± 7	3.012	21	0.48	–	1.799
9	27.39	22 ± 6	2.875	22	0.35	–	1.758
10	18.82	14 ± 5	2.742	23	0.20	–	1.727
11	13.45	–	2.619	24	0.12	–	1.726
12	9.93	–	2.503				

[a] Theoretical data from ref.[1]; [b] experimental data from ref.[2].

conditions in both the calculations and the PIES experiment just mentioned correspond to thermal energies. At these energies, the autoionization process in this type of a system is best looked upon as proceeding in two microscopic steps[3,4]. In the first step,

$$A^* + BC \rightarrow [A\ldots BC^+] + e\ , \qquad (2a)$$

the system leaks into the continuum and, under the framework of the Miller[5] and Nakamura[6,7] theory of Penning ionization, undergoes a vertical transition from the Born–Oppenheimer resonant surface $V^*_{BO}(\boldsymbol{R})$ to the ionic one, V^+_{BO} $(\boldsymbol{R})$. In the second step, the collision continues on the ionic surface

$$\begin{aligned} [A\ldots BC^+] &\rightarrow BC^+ + A \\ &\rightarrow AB^+ + C \\ &\rightarrow (ABC)^+ \\ &\rightarrow A + B^+ + C\ . \end{aligned} \qquad (2b)$$

Here the products represent, respectively, the Penning, rearrangement, associative and dissociative channels.

The ultimate goal of a theoretical description of an A* + BC collision system is to get an information about the product branching, step (*2b*), of the collision process. For He^*–D_2, the total ionization cross section and product branching were measured[8], and an experimental information about their collision energy dependence has also been reported[8]. There is no doubt that in addition to their importance for an interpretation of the PIES measurements, the vibrational populations of the nascent Penning ions $BC^+(v')(\ldots A)$ represent an important attribute of the initial conditions[2,3] of the step (*2b*) of the autoionization process. On the other hand, it is not clear whether a physically relevant description of the PIES characteristics themselves is not only a necessary but also a sufficient condition for an adequate description of the starting conditions for a 3D classical trajectory treatment of the step (*2b*) of the collision process. In particular, one can wonder whether the rate of convergence with the number of trajectories run of more detailed dynamical features of the set of final states of the vertical transitions from the resonant to the ionic surface is not significantly slower than that corresponding to the PIES characteristics. In view of this and with an eye to future attempts at theoretical interpretation of the product branching in the $He(2^3S)$–$D_2(H_2,HD)$ collision systems, it appears desirable to gain a deeper insight into convergence properties of the

Monte Carlo quasiclassical trajectory calculations on atom–diatom autoionizing collision systems with repulsive interaction.

The purpose of this paper is to present and discuss results of calculations of this type for the autoionization event in the $He(2^3S)–D_2(v'' = 0)$ collision system.

CALCULATIONS

As in our earlier paper[1], the present calculations are performed with the use of a two-dimensional (2D) classical trajectory model of the dynamics of the ionization event in thermal energy collisions in autoionizing A* + BC systems with repulsive interactions[9]. In low energy collisions in systems of this class, the BC^+ molecule-ion formed in step (*2a*) is only slightly perturbed by the A collision partner. As a consequence, the most prominent quantum features of the ionization event which exhibit themselves in the vibrational structure of the corresponding Penning electron spectra are generally connected with the vibrational motion of the perturbed $BC^+(v')(\ldots A)$.

The main motivation behind the approach of ref.[9] was to adopt this view and adequately describe the above quantum features of the ionization event, without loosing the possibility of following the dynamics of the rather complicated step (*2b*) of the collision process. For the stage of the collision process before the ionization event A* + $BC(v'') \rightarrow [A\ldots BC^+(v')]$ + e takes place, a separate quantum mechanical treatment of the perturbed $BC(v'')$ $[BC^+(v')]$ vibrational motion is adopted in the model and included into the calculation of static characteristics of the system. These characteristics thus depend on the distance R from A* to the center of mass I of the BC collision partner, the (AI, BC) angle γ and the pertaining vibrational quantum numbers of the perturbed BC and BC^+. In the dynamical part of the description of this stage of the process, the BC collision partner is treated as a rigid rotor.

The necessary analytical representations of the 2D surfaces for the resonant energy $D_2(v'' = 0)(\ldots He^*)$, the $D_2^+(v')(\ldots He)$ vibrational population factors and the energy of the corresponding Penning electrons for the ionization event were obtained from the values of the 2D static characteristics of the system calculated in our previous work[10]. These 2D characteristics were in turn obtained from the 3D Born–Oppenheimer surfaces.

In the approach of ref.[9], the motion of the system (with the D_2 collision partner treated as a rigid rotor) is governed by the potential $V^*_{v''}(R,\gamma)$ where v'' denotes the vibrational quantum number of the perturbed $D_2(\ldots He^*)$ diatomic. Information about the value of this potential for R, γ is obtained[11] from the one-dimensional Schrödinger equation

$$-\frac{\hbar^2}{2\mu}\frac{\mathrm{d}^2\chi_v(R,\gamma; r)}{\mathrm{d}r^2} + \left(V^j_{\mathrm{BO}}(R,\gamma; r) - V^j_v(R,\gamma)\right)\chi^j_v(R,\gamma; r) = 0 \quad . \qquad (3)$$

Here μ is the reduced mass of the D_2 pair, the superscript *j* becomes * for the resonant surface, and $V^*_{BO}(R,\gamma; r)$ is the 3D Born–Oppenheimer resonant potential.

It should be noted that in refs[9,11] the 2D resonant potential was allowed to be dependent on the end-over-end rotational quantum number *N* of the perturbed diatomic collision partner. In this work the dependence on *N* of the static characteristics, including the resonant potential is ignored[1]. The local widths of the He(2^3S)–D_2 system which, in addition to the resonant 2D surface, determine the behaviour of the system with respect to autoionization to $D_2^+(v')$(…He), are given by the expression

$$\Gamma(v'',v'; R,\gamma) = | \langle \chi^*_{v''}(R,\gamma; r)| [\Gamma_{BO}(R,\gamma; r)]^{1/2} | \chi^+_{v'}(R,\gamma; r) \rangle_r|^2 \quad . \qquad (4)$$

This expression was found in the calculations[9,11,12] on He(2^3S)–H_2 to provide physically more relevant picture of the autoionization event than simpler local Franck–Condon factors. The $\chi^+_{v'}(R,\gamma; r)$ wavefunction corresponds to the final state of the event (2a) and is an eigenfunction of the Schrödinger equation (*3*) for the ionic potential (*j* = +), $\Gamma_{BO}(R,\gamma; r)$ is the Born–Oppenheimer width of the He(2^3S)–H_2 resonant state. In the analytical representation of all the 2D surfaces, the angular dependence of the characteristics is accounted for by a truncated (*l* = 0, 2, 4, 6) Legendre expansion and the *R* dependence of the Legendre components is described by cubic taut-spline fits[13].

The trajectory calculations are performed using our FORTRAN code based on Hamilton's equations given in ref.[9], with the proviso that a dependence of the resonant potential (and of the local width of the state with respect to autoionization) on the end-over-end rotational quantum number *N* of D_2(…He*) is not considered. The way of calculating the 2D trajectories is in this approach quite intentionally chosen to closely correspond to the 3D approach of Karplus, Porter and Sharma[14], adopted in the modified trajectory surface leaking (TSL) scheme[15,16]. The state of the system is described by five general coordinates and the momenta conjugate to them: two of the coordinates are the angles θ and φ which specify the orientation (with respect to a fixed laboratory frame) of the line joining the centre B to C. The remaining coordinates Q_1, Q_2, and Q_3 are the Cartesian coordinates of the collision partner A* with respect to the centre of mass of the BC pair. The conjugate momenta to these general coordinates are

$$P_\theta = \mu_{BC}\, l^2 \dot{\theta}$$

$$P_\phi = \mu_{BC}\, l^2 \sin^2\theta \dot{\phi}$$

$$P_i = \mu_{A,BC}\, \dot{Q}_i \quad (i = 1, 2, 3) \quad , \qquad (5)$$

where l is the (fixed) BC distance, μ_{BC} is the reduced mass of the BC pair and $1/\mu_{A,BC} = 1/m_A + 1/(m_B + m_C)$.

The values of the general coordinates and their conjugate momenta at the beginning of the trajectories are chosen in essentially the same way as in ref.[1]. The values of the collision variables at the beginning of the trajectories are taken to correspond to the realistic distribution of the rotational states J of D_2 at 300 K. More specifically, the distribution of rotational states is computed from the expression

$$F_{BC}(J,v'' = 0) = \frac{f_J(2J + 1) \exp(-E_{v''=0,J}/kT)}{Q_{v''=0,J}} , \qquad (6)$$

where $Q_{v'' = 0,J}$ is the rotation-vibration partition function, $E_{v'' = 0,J}$ is the energy of the state (derived from the data given in ref.[17]), and f_J is its nuclear statistical weight (in D_2, $f_J = 6$ for even J and $f_J = 3$ for odd J). The impact parameter b was randomized in the range $0 \le b < 9$ a.u. The choice of this rather large maximal value of b, b_{max}, is dictated by the R dependence of the $\Gamma_{BO}(R,\gamma; r)$ surface[15,16,18,19] which makes the probability of ionization of the system negligible only for trajectories with large impact parameters. The trajectories started at $R_0 = 10$ a.u. As far as the initial collision energy is concerned, two sets of calculations were carried out. In the first set, which is an extention of the work of ref.[1], the energies range from 10 to 150 meV with an average of 51 meV, the distribution simulating the experimental one in the PIES measurements of ref.[20]. In the second set of calculations, the starting collision energy was kept fixed at the value of 50 meV. The initial values of the remaining variables were selected in the same way as in ref.[14]. The DD distance was fixed at 1.41408 a.u. The length of the numerical integration time step was kept fixed at 7.5 a.u. This value proved to be small enough to ensure a sufficiently accurate integration of the equations of motion of ref.[9] and an adequate treatment of the ionization event. As far as this treatment is concerned, we here only note that at each integration time step i in the trajectory, the probability $P(R_i,\gamma_i)$ of leaking of the system into the continuum is computed from the expression[9,21]

$$P(R_i,\gamma_i) = \frac{\sum_{v'=0} \Gamma(v'',v'; R_i,\gamma_i)}{\hbar} \Delta t_i , \qquad (7)$$

where Δt_i is the length of the numerical integration time step. A pseudorandom number ζ_i is then generated and compared with this probability. If $P(R_i,\gamma_i) \le \zeta_i$, the trajectory continues on the resonant surface. If $P(R_i,\gamma_i) > \zeta_i$, however, an electron is ejected and the system leaks into the continuum. The determination of the vibrational state of the nascent Penning ion formed in the transition is based on a comparison of an extra pseudorandom number ζ_{tr} with the set of (appropriately normalized) local widths for the transition (*1*) taking place at the configuration of the system corresponding to the inte-

gration time step of the ionization. Once the quantum number v' is determined, one calculates the energy of the Penning electron released in the transition as the difference between the pertinent eigenenergies of the Schrödinger equation (*3*)

$$E_{v'}(R,\gamma) = V^{*}_{v''=0}(R,\gamma) - V^{+}_{v'}(R,\gamma) \quad . \tag{8}$$

Further, the actual value of $V^{+}_{v'}(R,\gamma)$, together with the corresponding 1D cut through the 3D Born–Oppenheimer ionic potential $V^{+}_{BO}(R,\gamma; r)$, the actual values of the corresponding general coordinates and their conjugate momenta[9] can be used to specify the starting conditions for the rest (stage (*1b*)) of the trajectory. Of course, the starting value of the phase of the $BC^{+}(v')(\ldots A)$ vibrational motion will have to be randomized with the help of an additional pseudorandom number.

RESULTS AND DISCUSSION

As a brief introduction to this section we wish to stress that because of low collision energies in Penning ionization calculations (and experiments), repulsive character of the atom–diatom system studied here, and very small magnitude of the values which the local widths can take on along the trajectories, only a very small fraction of the trajectories started on the resonant surface leads to the autoionization (*2a*). As indicated in the previous section, the state of each of the 2D trajectories found to lead to ionization can be described by the vibrational quantum number v', the energy of the released electron $E_{v'}(R,\gamma)$ and the values at the autoionization event of the five above mentioned general coordinates and their conjugate momenta (*5*). Thus, at the autoionization event a trajectory (leading to ionization) is in the present approach characterized by a 12-fold entity with the components just mentioned. A set of these 12-fold entities for all the trajectories found in the course of the calculations to lead to ionization forms a 2D classical trajectories picture of the autoionization event.

It is clear from what has been indicated above that, in general, it is necessary to run a large number of trajectories on the resonant potential surface to adequately describe the final state of the ionization event. On the other hand, the requirements on the level of completeness of the classical trajectory picture of the event depend on the purpose of the calculations. If the aim of the calculations is limited to provide an information about the total ionization cross section, then, roughly speaking, only the ratio of the number of ionized trajectories to the number of those started on the resonant surface is essential. When a PIES spectrum corresponding to the step (*2a*) of the process is to be interpreted, it is necessary to extend considerations to the numbers of trajectories labelled by individual quantum numbers v' and to the energies of the released electrons $E_{v'}(R,\gamma)$. In those situations where one wishes to treat the stage (*2b*) of the collision process, the set of the ionized trajectories should also provide an adequate repre-

sentation of the set of those components of the 12-fold entities which correspond to the above mentioned general coordinates and their conjugate momenta (*5*). This should be done not only for the whole set of the ionized trajectories but also for each subset, corresponding to each of the most populated individual vibrational levels v' of the nascent Penning ion [A*…$BC^+(v')$]. The most challenging situation for a theoretical description of the autoionization step (*2a*) would arise if one would wish to interpret electron-ion coincidence experiments on an A*–BC autoionization system, in which the product branching ratio for individual vibrational states of the nascent Penning ion formed in the step (*2a*) is measured[4]. In this case, one should ideally get a realistic representation of the part of the 12-fold entities related to the general coordinates and their conjugate momenta (*5*) for the subsets corresponding to each of the individual vibrational levels v' of the nascent Penning ion.

Let us turn now our attention to Fig. 1 in which we show an approximation to the total ionization cross section for the $He(2^3S)$–D_2 collision system as a function of the number of the trajectories run *N*. The approximation was calculated from the expression[14]

$$\sigma = \pi b_{\max}^2 N_i / N \ , \qquad (9)$$

where $b_{\max}$, the maximal impact parameter, was taken to be 9 a.u. (see above), and N_i is the number of the trajectories leading to ionization. The calculations of the total ionization cross section represent an extension of one of the batches of the trajectories discussed in ref.[1]; the initial collision energy ranges from 10 to 150 meV (average of about 51 meV). It can be seen from this figure that for $N > 2\ 500\ 000$, the changes in the total ionization cross section with increasing number of the trajectories run are

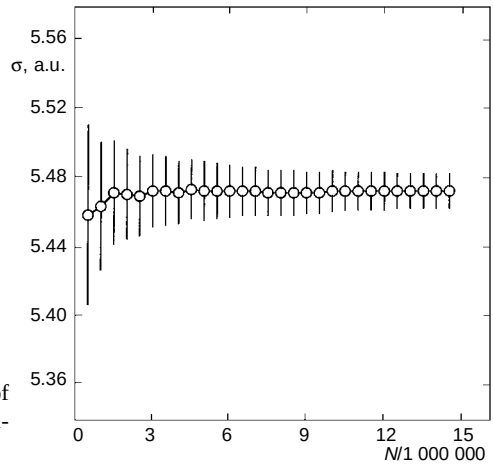

FIG. 1
Total ionization cross section as a function of the number of the trajectories run. The vertical lines represent standard errors

already very small. Hence, at 2 500 000 trajectories which formed a basis for the study of our work[1], the value of the total ionization cross section is very well converged. It should be noted that of this portion of the trajectories, 53 744 (2.15%) trajectories were found to lead to ionization, the corresponding approximation to the total cross section being $(5.470 \pm 0.032)a_0^2$. At 14 552 000 trajectories, these quantities were found to converge, respectively, to 312 864 (2.150%) and $(5.471 \pm 0.010)a_0^2$. The magnitude of the changes as well as the shape of the curve in Fig. 1 suggest that for the collision conditions studied, even 500 000 trajectories might suffice for most purposes. In this case, the number of the ionized trajectories amounts to 10 726 (2.145%) and the total cross section is $(5.459 \pm 0.052)a_0^2$.

The rest of the study is based on the set of calculations with the initial collision energy fixed at 50 meV. As already indicated in the previous section, this set of calculations was finished with a batch of 10 000 000 trajectories. Of these, 200 653 (2.007%) trajectories were found to lead to ionization. The corresponding total ionization cross section is $(5.106 \pm 0.011)a_0^2$. Table II presents average energies of the Penning electrons corresponding to individual vibrational levels of the nascent Penning ion $[He\ldots D_2^+(v')]$. The values are averages of the values (*8*) taken over the first N_i ionized trajectories indicated in the table, and are related to the position of the corresponding peaks in the Penning electron spectra. It can be seen from this table that for $v' > 3$, roughly speaking, the rate of convergence of the $E_{v'}$ values with N_i decreases with the increasing vibrational level of the nascent Penning ion v'. One of the consequencies of this fact can be seen in Table II at the level of approximation corresponding to 10 000 ionized trajectories, where the average Penning electron energy for the final state vibrational level $v' = 23$ is greater than that predicted for the state $v' = 22$. The overall situation is illustrated by Fig. 2 in which we show the $E_{v'}$ *vs* N_i dependence for the vibrational levels $v' = 3$, 13, and 20 of the nascent Penning ion. The decreased rate of convergence for high v' reflects the fact that the fraction of the ionized trajectories which correspond to high v' levels of the nascent Penning ion is exceedingly small (*cf.* Tables I and III). As a consequence, in order to collect sufficiently large number of the ionized trajectories with high v' to get a satisfactory statistics for the corresponding vibrational level, it is necessary to perform much more extended calculations than in the case of the levels with high population factors. It should be noted in this connection that this feature of the autoionization event in the system exhibits itself also in uncertainties in the experimental results of ref.[2] reproduced in Table I. In spite of this we can conclude that, provided one does not insist on describing subtleties of an accurate description of the Penning electron energies for high v', the average electron energies obtained from 40 000 ionized trajectories or so might be acceptable. On the other hand, the gross overall features of the set of average Penning electron energies appear to be adequately represented by the trajectory calculations with 20 000 ionized trajectories.

While the average Penning electron energies are related to the eigenvalues of the Schrödinger equation (*3*) for the perturbed D_2(…He*) and D_2^+(…He), the local widths of the He(2^3S)–D_2 system with respect to autoionization (*4*) and, hence, the vibrational

TABLE II
Average Penning electron energies $E_{v'}$ (in eV) in autoionization event He(2^3S) + $D_2(v'' = 0) \rightarrow$ [He…D_2^+] + e as a function of the different number of the ionization trajectories N_i

v′	$E_{v'}$						
	N_i = 5 000	N_i = 10 000	N_i = 20 000	N_i = 50 000	N_i = 100 000	N_i = 150 000	N_i = 200 653
0	4.372	4.372	4.372	4.373	4.373	4.373	4.373
1	4.174	4.174	4.174	4.174	4.174	4.174	4.174
2	3.985	3.985	3.985	3.985	3.985	3.985	3.985
3	3.803	3.803	3.803	3.803	3.803	3.803	3.803
4	3.629	3.629	3.629	3.629	3.629	3.629	3.629
5	3.463	3.462	3.462	3.463	3.463	3.463	3.463
6	3.304	3.304	3.304	3.304	3.304	3.304	3.304
7	3.152	3.152	3.152	3.152	3.152	3.152	3.152
8	3.007	3.007	3.007	3.007	3.007	3.007	3.007
9	2.869	2.869	2.869	2.869	2.869	2.870	2.870
10	2.738	2.737	2.737	2.738	2.739	2.739	2.739
11	2.616	2.615	2.615	2.614	2.615	2.615	2.615
12	2.497	2.497	2.498	2.497	2.497	2.497	2.498
13	2.383	2.385	2.386	2.387	2.387	2.387	2.387
14	2.287	2.287	2.287	2.286	2.286	2.286	2.285
15	2.187	2.188	2.188	2.190	2.190	2.190	2.190
16	2.101	2.101	2.102	2.100	2.102	2.101	2.101
17	2.019	2.017	2.017	2.019	2.021	2.021	2.022
18	1.948	1.953	1.952	1.951	1.950	1.949	1.949
19	1.887	1.884	1.883	1.883	1.883	1.883	1.884
20	1.824	1.825	1.832	1.830	1.831	1.830	1.831
21	1.776	1.779	1.779	1.785	1.784	1.781	1.783
22	1.721	1.721	1.731	1.748	1.751	1.750	1.750
23	1.703	1.728	1.720	1.734	1.730	1.728	1.725
24	1.702	1.714	1.714	1.706	1.709	1.707	1.712

population factors for the nascent Penning ion $P_{v'}$ are related to 1D vibrational wave functions of the perturbed diatomic collision partners. It is well known that eigenfunctions are more sensitive to perturbations than the corresponding eigenvalues. As a consequence, the changes in the local widths of the $He(2^3S)$–D_2 collision system caused by changes in the $He(2^3S)$–D_2 configuration are, in general, more significant than those encountered in the Penning electron energies (*8*). One can therefore expect that the rate of convergence of the (dynamical) nascent vibrational populations will be lower than that found for the averaged Penning electron energies. Indeed, this overall tendency is seen in Table III, where we give data about the values of the nascent vibrational populations as obtained at different stages of the trajectory calculations and in Fig. 3 in which we illustrate the situation for 3 selected vibrational levels of the nascent Penning ion. Note that at 20 000 ionized trajectories, the order of the population factors for the vibration levels $v' = 22$ and 23 is still reversed. At 50 000 ionized trajectories, the situation is in this respect correct and the gross overall features of the set of the nascent

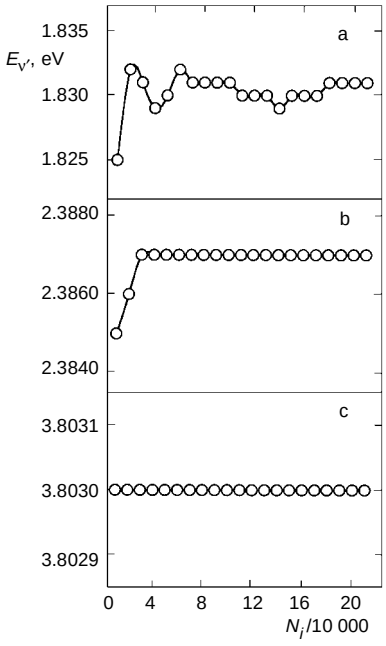

FIG. 2
Average Penning electron energies at the ionization event $He(2^3S)$–$D_2 \rightarrow [He\ldots D_2^+]$ + e as a function of the number of the ionized trajectories for three selected vibrational levels: a $v' = 20$; b $v' = 13$; c $v' = 3$

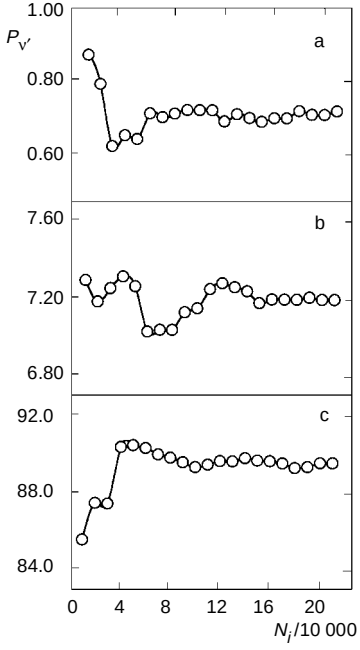

FIG. 3
Vibrational population factors (normalized to 100 at $v' = 3$) at the ionization event $He(2^3S)$–$D_2 \rightarrow [He\ldots D_2^+]$ + e as a function of the number of the ionized trajectories for three selected vibrational levels: a $v' = 20$; b $v' = 13$; c $v' = 2$

vibrational population factors are already described adequately. We can therefore conclude that as far as the interpretation of PIES measurements in the $He(2^3S)$–D_2 system at the collision energy of 50 meV is concerned, the main features of the spectra are

TABLE III
Vibrational population factors $P_{v'}$ (normalized to 100 at $v' = 3$) in autoionization event $He(2^3S) + D_2(v'' = 0) \rightarrow [He\ldots D_2^+] + e$ as a function of the different number of the ionization trajectories N_i

v′	$P_{v'}$						
	N_i = 5 000	N_i = 10 000	N_i = 20 000	N_i = 50 000	N_i = 100 000	N_i = 150 000	N_i = 200 653
0	24.90	25.60	24.77	26.17	25.61	25.90	25.67
1	58.46	58.49	61.19	62.88	63.12	62.73	62.75
2	82.16	85.50	87.43	90.42	89.32	89.68	89.57
3	100.00	100.00	100.00	100.00	100.00	100.00	100.00
4	94.81	89.37	92.59	94.75	94.47	92.80	92.69
5	75.50	77.27	78.82	80.49	79.90	79.79	79.77
6	61.92	61.77	62.45	63.93	63.66	63.74	64.34
7	49.27	49.53	50.15	50.95	50.37	49.45	49.79
8	34.09	34.56	34.03	37.11	36.29	36.08	36.44
9	24.10	23.80	26.99	27.78	26.94	26.80	26.86
10	16.91	17.65	17.73	18.82	18.98	18.93	18.97
11	11.85	12.30	13.32	13.67	13.32	13.50	13.28
12	8.12	8.89	9.36	9.90	10.03	10.03	9.90
13	7.59	7.29	7.18	7.26	7.15	7.18	7.20
14	5.06	4.75	5.33	4.81	4.77	4.77	4.88
15	2.80	2.94	3.35	2.96	3.24	3.32	3.31
16	2.26	2.67	2.63	2.68	2.62	2.62	2.62
17	1.47	1.60	1.71	1.70	1.91	1.91	1.87
18	1.47	1.27	1.40	1.39	1.32	1.35	1.40
19	0.93	1.00	0.96	1.00	1.01	0.94	0.90
20	0.53	0.87	0.79	0.64	0.72	0.69	0.72
21	1.07	0.87	0.65	0.59	0.49	0.48	0.47
22	0.13	0.07	0.14	0.29	0.29	0.27	0.24
23	0.27	0.20	0.24	0.22	0.20	0.18	0.19
24	0.13	0.20	0.10	0.10	0.10	0.12	0.11

correctly represented by the 2D classical trajectory calculations leading to 50 000 ionized trajectories. When the calculations are extended so as to make it possible to interpret the PIES spectra on the basis of 100 000 ionized trajectories, the overall situation with regard to the pertinent quantities is further improved and, taking into account the present state of the art on the experimental side, the degree of convergence for these quantities can be considered to be very satisfactory.

Let us turn our attention to that portion of the starting conditions for the 3D classical trajectory treatment of the postionization step (*2b*) which is not directly connected with the quantum number v' of the nascent Penning ions [He…$D_2^+(v')$]. It should be noted that the set of the actual values of the corresponding general coordinates and their conjugate momenta[1] specifies starting conditions for a classical trajectory description of the rest of the process. The set of these quantities formed by all the ionized trajectories creates a phase space. Strictly speaking, for a physically relevant description of the postionization step, the distribution functions in the phase space for individual vibrational levels should be identical with the overall distribution (sum over all the vibrational levels).

For simplicity we have decided not to present an analysis of the sets of the general coordinates and of their (in some cases rather abstract) conjugate momenta. Rather, we shall work with two derived quantities, with an evident importance for a classical trajectory description of the initial conditions of the second step of the collision process. The first quantity is the distance R from He to the midpoint of the D_2^+ collision partner and the second one is a relative kinetic energy of the He–D_2^+ motion.

In Fig. 4 we show an overall distribution of the distance R at the ionization event as obtained from the trajectory calculations leading to different numbers of the ionized trajectories N_i. The distributions are seen to reflect the fact that the resonant surface $V^*_{BO}(R,\gamma;r)$ and, consequently, the 2D surface $V^*_{v'=0}(R,\gamma)$ is repulsive and that, for a given Δt_i and a fixed angle γ, the probability of ionization (*7*) increases exponentionally with decreasing R_i. Note that the initial collision energy was kept fixed at 50 meV in these calculations. It can be seen from this figure that at the number of ionized trajectories N_i = 50 000, the overall distribution is already not too far from that we obtained at the final stage of our calculations. A similar rate of convergence is seen from Fig. 5 to occur for the R distribution corresponding to the nascent Penning ion [He…$D_2^+(v')$] with the most populated vibrational level v' = 3. The situation corresponding to the vibrational level v' = 20 which is much less populated than the v' = 3 one (*cf.* Tables I and III) is different. It is seen from the corresponding panel of Fig. 5 that the rate of convergence is considerably slower than in the v' = 3 case. Concomitantly, the final approximation to the R distribution for this vibrational level of the nascent Penning ion (based on 207 ionized trajectories) must be judged inferior to the v' = 3 one.

Figure 6 shows an overall distribution of the He–D_2^+ relative kinetic energy E_k at the ionization event (*1*) as obtained from the same stages of the trajectory calculations

discussed above in the case of the R distributions. The negative and positive signs represent the direction of the relative motion of the He collision partner to the $D_2^+(v')$ ion at the autoionization event. The negative sign corresponds to the situations where the autoionization event takes place when the collision partners are approaching each other while the positive sign denotes receding collision partners at the autoionization event. Figure 7 is an E_k distribution analogue of Fig. 5. A comparison of Figs 6 and 7 with their R distribution counterparts leads us to conclude that as far as the rate of convergence of the E_k distribution is concerned, the situation is, for all the individual vibrational levels of the nascent Penning ion considered very similar to that encountered in the case of the R distribution. The same is true with regard to the level of accuracy of the final approximation to the E_k distributions we obtained for the individual vibrational levels of the nascent Penning ion $[He\ldots D_2^+(v')]$.

The above considerations suggest that in the present 2D classical trajectory model of the autoionization event, some 2 000 ionized trajectories could already form a satisfactory basis for a physically acceptable distribution of each of those continuous components of the 12-fold ionized trajectory entities which are not directly related to the quantum number v' of the corresponding nascent Penning ion. It should be stressed that in the batch of trajectories with the sharp initial collision energy of 50 meV, we calculated as huge a number of trajectories as 10 000 000. In spite of this, of the individual

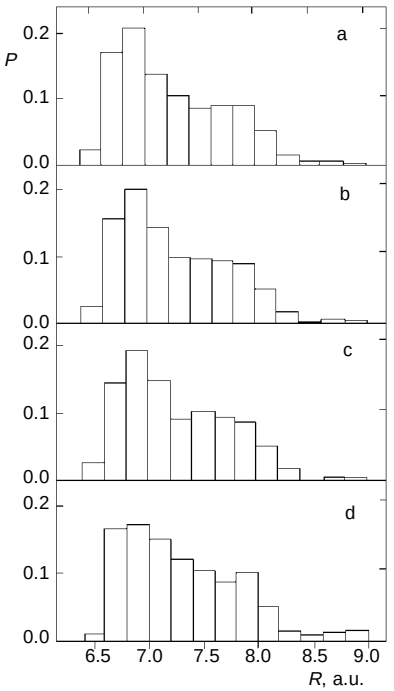

FIG. 4
Histogram of the overall distribution, P, of the R_{He-D_2} distance at the ionization event $He(2^3S)–D_2 \rightarrow [He\ldots D_2^+] + e$ for four selected numbers of the ionized trajectories: a N_i = 200 653; b N_i = 100 000; c N_i = 50 000; d N_i = 1 000

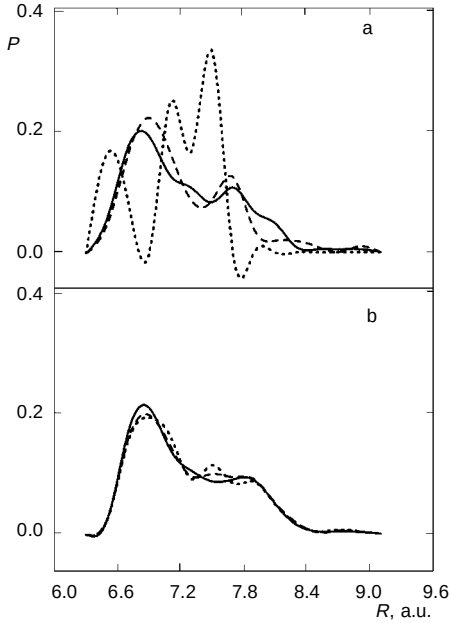

FIG. 5

Distribution P of the $R_{He–D_2}$ distance at the ionization event $He(2^3S)–D_2 \rightarrow [He…D_2^+] + e$ for two selected vibrational levels: a $v' = 20$; b $v' = 3$ for three different numbers of the ionized trajectories. Dot line represents 10 000, dash line 100 000, and full line 200 653 ionized trajectories

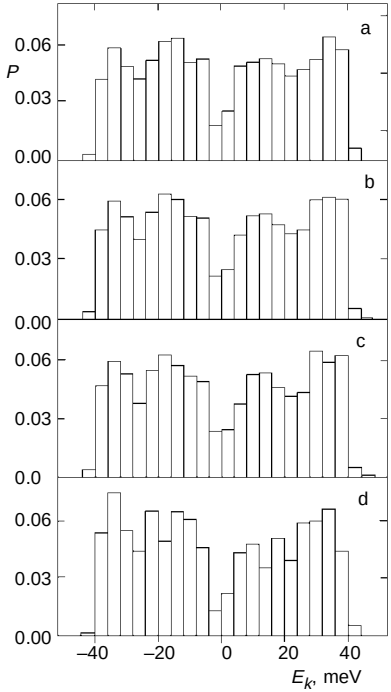

FIG. 6

Histogram of the overall distribution, P, of the $He–D_2^+$ relative kinetic energy at the ionization event $He(2^3S)–D_2 \rightarrow [He…D_2^+] + e$ for four selected numbers of the ionized trajectories: a N_i = 200 653; b N_i = 100 000; c N_i = 50 000; d N_i = 1 000

vibrational levels of the nascent Penning ion populated, we were able to reach this limit only for the vibrational levels with $v' \leq 13$. An estimate of the scale of the calculations, required to get a similar level of approximation to the distributions for higher vibrational levels of the nascent Penning ions, can be obtained from the vibrational population factors of Table III. This leads us to conclude that an accurate interpretation of the electron–ion coincidence measurements would require very demanding large-scale trajectory calculations. On the other hand, one must bear in mind that the rapid decrease with the increasing v' level of the nascent population factors causes problems not only in a theoretical description of subtle aspects of the autoionization event in the system connected with the high v' levels of the nascent Penning ion but also in experiments. As examples we can mention the uncertainties in the high v' tails of experimental data in the Penning electron spectra[2] of He(2^3S)–D_2 and missing information in the electron-ion coincidence measurements on the HH isotopic variant of the system[4]. With this problems on both the theoretical and experimental sides, some of the above conclusions concerning the subtle aspects of the autoionization to high v' levels of the nascent Penning ions should be regarded as plausible rather than conclusive. In view of this we also consider it best to leave the questions of the adequacy of the approximation to the 2D classical trajectory picture of the autoionization event open until the present data is used as an input for 3D classical trajectory description of the step (*2b*) of Penning ionization for individual vibrational levels of the nascent Penning ions [He…$D_2^+(v')$].

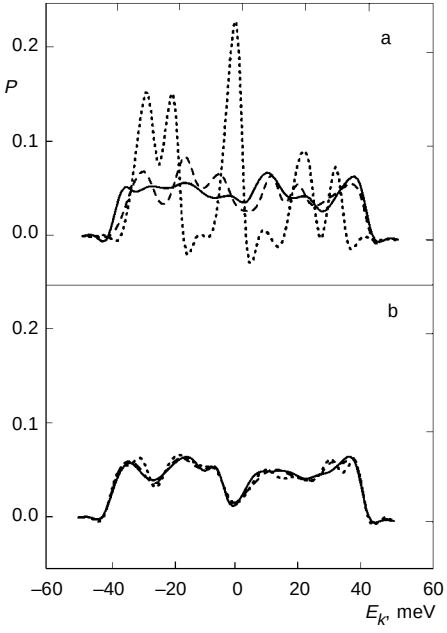

FIG. 7
Distribution P of the He–D_2^+ relative kinetic energy at the ionization event He(2^3S)–D_2 → [He…D_2^+] + e for two selected vibrational levels: a $v' = 20$; b $v' = 3$ for three selected numbers of the ionized trajectories. Dot line represents 10 000, dash line 100 000, and full line 200 653 ionized trajectories

CONCLUDING REMARKS

The discussion of the previous section was based on the calculations for the relative collision energy of 50 meV. Estimates of the level of accuracy of the approximation achieved were made for different numbers of the ionized trajectories N_i and some conclusions were made in terms of the ionized trajectories with the vibrational level under question. The total number of the trajectories run N was more or less considered implicitly.

Consider now a picture of the autoionization event in the present system corresponding to a different collision energy in a range from 20 to 150 meV. According to the recent work[12] on the collision energy dependence of the autoionization event in the HH… isotopic variant of the present system, all the main conclusions of this work will remain valid. Of course, the numbers of the trajectories N which have to be run on the resonant surface to get a given number of the ionized trajectories N_i will differ from the present one. If a value of the total ionization cross section for the collision conditions is known from other sources, *e.g.*, from experiment, then an estimate of the actual number N corresponding to the number of the ionized trajectories N_i can be obtained from Eq. (*9*). Otherwise, as shown in the previous section, an acceptable estimate of the N_i/N ratio can be obtained already from sample calculations which are not too much time consuming.

The arguments and conclusions of the previous section were based on the 2D classical trajectory calculations on the He(2^3S)–D_2 system, which serves as a representative of an atom–diatom autoionizing collision system with a repulsive interaction. It seems natural to rise a question if the present results can be of any value for an assessment of the convergence properties of analogous 2D classical trajectory calculations on an atom–diatom collision system of this class. The answer is affirmative. Certainly, in addition to the total ionization cross section, most of the arguments of the previous section is quite closely connected with the number of the vibrational levels of the nascent Penning ion and, with their population factors. As a consequence, there is no problem to get an idea about the convergence properties of the trajectory description of the autoionization event for those A*–BC collision systems, where an information about the total ionization cross section is available and at least some approximation to the nascent population factors is at hand. From this point of view one can consider four different types of approximation:

1. The nascent vibrational population factors are known from precise experiments. As an example we can mention the very precise PIES data for the He*–H_2 system[20].

2. The vibrational population factors are known from dynamical calculations. The only example known to the authors is the He(2^3S)–H_2 system with the vibrational levels up to $v' = 16$ (refs[9,12]).

3. The vibrational population factors can be deduced from the local widths (*4*) of the system with respect to autoionization. An example[23] is the He(2^3S)–HD system with the vibrational levels up to $v' = 19$.

4. In those situations where only the total ionization cross section for the A*–BC system with repulsive interaction is available, gross features of the convergence properties of a 2D classical trajectory description of the autoionization event can be obtained with the help of the Franck–Condon factors for the isolated diatomic collision partner[20,11].

The work was sponsored partly by the Grant Agency of the Czech Republic (Grant No. 203/95/1055) and partly by the European Network (Human Capital and Mobility Program) "Structure and Reactivity of Molecular Ions".

REFERENCES

1. Vojtik J., Kotal R.: Chem. Phys. Lett. *255*, 251 (1996).
2. Bevsek H. M., Dunlavy D. C., Siska P. E.: J. Chem. Phys. *102*, 133 (1995).
3. Hotop H., Niehaus A.: Z. Phys. *215*, 395 (1968).
4. Münzer A., Niehaus A.: J. Electron Spectrosc. Relat. Phenom. *23*, 367 (1981).
5. Miller W. H.: J. Chem. Phys. *52*, 3562 (1970).
6. Nakamura H.: J. Phys. Soc. Jpn. *26*, 1473 (1969).
7. Nakamura H.: J. Phys. Soc. Jpn. *31*, 574 (1971).
8. Martin D. W., Weiser C., Sperlein R. F., Bernfeld D. L., Siska P. E.: J. Chem. Phys. *90*, 1564 (1989).
9. Vojtik J.: Chem. Phys. Lett. *214*, 425 (1993).
10. Vojtik J., Kotal R.: J. Phys. Chem. *99*, 15473 (1995).
11. Vojtik J.: Chem. Phys. *170*, 209 (1993).
12. Vojtik J.: Chem. Phys. *209*, 367 (1996).
13. de Boor C.: *A Practical Guide to Splines*. Springer, Berlin 1978.
14. Karplus M., Porter R. N., Sharma R. D.: J. Chem. Phys. *43*, 3259 (1965).
15. Vojtik J., Paidarova I.: Chem. Phys. *157*, 67 (1991).
16. Vojtik J.: Laser Chem. *11*, 187 (1991).
17. Bredohl H., Herzberg G.: Can. J. Phys. *51*, 867 (1973).
18. Vojtik J., Paidarova I.: Chem. Phys. Lett. *99*, 93 (1983).
19. Vojtik J., Paidarova I.: Chem. Phys. Lett. *103*, 305 (1983).
20. Bregel T., Yencha A. J., Ruf M.-W., Waibel H., Hotop H.: Z. Phys. D *13*, 51 (1989).
21. Preston R. K., Cohen J. S.: J. Chem. Phys. *65*, 1589 (1976).
22. Penton J. R., Muschlitz E. E.: J. Chem. Phys. *49*, 49 (1968).
23. Vojtik J.: Int. J. Quantum Chem. *57*, 543 (1996).